Published in final edited form as:
Neuroimage. 2011 February 1; 54(3): 1887–1895. doi:10.1016/j.neuroimage.2010.10.027.

β-amyloid affects frontal and posterior brain networks in normal aging

Hwamee Oh[a,*], **Elizabeth C. Mormino**[a], **Cindee Madison**[a], **Amynta Hayenga**[a], **Andre Smiljic**[a], and **William J. Jagust**[a,b]

[a]Helen Willis Neuroscience Institute, University of California - Berkeley, Berkeley, CA 94720, USA

[b]Life Sciences Division, Lawrence Berkeley National Laboratory, Berkeley, CA 94720, USA

Abstract

Although deposition of β-amyloid (Aβ), a pathological hallmark of Alzheimer's disease (AD), has also been reported in cognitively intact older people, its influence on brain structure and cognition during normal aging remains controversial. Using PET imaging with the radiotracer Pittsburgh compound B (PIB), structural MRI, and cognitive measures, we examined the relationships between Aβ deposition, gray matter volume, and cognition in older people without AD. Fifty-two healthy older participants underwent PIB-PET and structural MRI scanning and detailed neuropsychological tests. Results from the whole-brain voxel-based morphometry (VBM) analysis revealed that gray matter volume in the left inferior frontal cortex was negatively associated with amyloid deposition across all participants whereas reduced gray matter volume was shown in the posterior cingulate among older people with high amyloid deposition. When gray matter density measures extracted from these two regions were related to other brain regions by applying a structural covariance analysis, distinctive frontal and posterior brain networks were seen. Gray matter volume in these networks in relation to cognition, however, differed such that reduced frontal network gray matter volume was associated with poorer working memory performance while no relationship was found for the posterior network. The present findings highlight structural and cognitive changes in association with the level of Aβ deposition in cognitively intact normal elderly and suggest a differential role of Aβ – dependent gray matter loss in the frontal and posterior networks in cognition during normal aging.

Keywords

Aging; Amyloid; PIB-PET; cognition; human; VBM

INTRODUCTION

β-amyloid (Aβ), a prominent feature of Alzheimer's disease (AD) pathology, is hypothesized to be an initiating factor in the pathophysiology of the disorder (Hardy et al., 2002; Jack et al., 2010). Accumulation of Aβ, however, has also been reported in cognitively

[*]Corresponding author. 132 Barker Hall MC #3190, University of California, Berkeley, CA, 94720-3190. Tel: +1 510 643 6616. Fax: +1 510 642 3192. hwameeoh@berkeley.edu (H. Oh).

intact older people (Aizenstein et al., 2008; Mintun et al., 2006; Rowe et al., 2007), although it remains unresolved whether and how Aβ deposition relates to other biological and cognitive factors in normal aging. Aβ deposition can now be measured in vivo with Pittsburgh Compound B (PIB) and positron emission tomography (PET) (Ikonomovic et al., 2008; Klunk et al., 2003, 2004). This study aimed to characterize the relationship between Aβ deposition measured by PIB PET and other features of AD, specifically gray matter loss and cognitive performance, and to assess the relationship between gray matter volume changes and cognitive performance in normal aging.

Brain atrophy is commonly observed in patients with AD and mild cognitive impairment (MCI) (Archer et al., 2006; Bobinski et al., 2000; Fotenos et al., 2005; Jack et al., 2002, 2008, 2009; Silbert et al., 2003). Results from cross-sectional studies have indicated a positive correlation between Aβ deposition and brain atrophy (Jack et al., 2008). Longitudinal studies have indicated that annual atrophy rates are positively associated with Aβ deposition (Archer et al., 2006; Jack et al., 2009; Scheinin et al., 2009) and the presence of clinical symptoms of AD (Fotenos et al., 2005). Among brain regions, the medial temporal lobe, especially hippocampus, is consistently reported as a region where atrophy is related to Aβ deposition, although other regions such as anterior/posterior cingulate, temporal cortices, precuneus, and frontal cortices are also affected (Braak & Braak, 1991; Csernansky et al., 2004; de Leon et al., 1989; Dickerson et al., 2009; Jack et al., 2008, 2009). Additional data suggest that clinical symptoms and cognitive performance are coupled to neurodegeneration measured by brain atrophy, but not to Aβ deposition (Jack et al., 2009; Dickerson et al., 2009).

The regional topography of Aβ deposition and gray matter volume loss has been shown to be largely overlapping. Functional connectivity studies have indicated that in patients with AD and MCI brain regions collectively known as the Default Mode Network (DMN) show reduced functional connectivity (Greicius et al., 2004; Sorg et al., 2007). The DMN is mostly comprised of the medial frontal cortex, posterior cingulate/precuneus, and bilateral parietal cortices. In AD and MCI patients, the same network has been identified as regions that accumulate Aβ (Buckner et al., 2005) and overlap with regional patterns of brain atrophy (Buckner et al., 2005; Sorg et al., 2007). Disrupted deactivation in the DMN has been related to poor episodic memory performance (Sperling et al., 2009). Thus, these findings may indicate that the same brain regions undergo both structural and functional changes in relation to Aβ deposition.

The association of Aβ deposition with gray matter volume has been reported not only in AD and MCI patients but also in cognitively intact normal elderly, showing an inverse relationship between PIB uptake and gray matter volume especially in hippocampus (Chetelat et al., 2010; Mormino et al., 2009). Mormino et al. (2009) showed that greater PIB uptake is significantly associated with reduced hippocampal volume in normal elderly and MCI. Chetelat et al. (2010) showed a similar pattern of association between PIB uptake and hippocampal gray matter volume in older subjects experiencing subjective cognitive impairments.

The relationships among Aβ deposition, gray matter volume, and cognition in normal aging, however, are yet unresolved. While some studies have shown a negative association between Aβ deposition and gray matter volume as well as episodic memory, others have shown no difference in gray matter volume or cognitive measures between elderly with evidence of Aβ accumulation and those without as seen with PIB (Aizenstein et al., 2008; Bourgeat et al., 2010; Jack et al., 2008; Pike et al., 2007; Reiman et al., 2009; Rowe et al., 2007). Furthermore, brain regions in which gray matter volume is associated with Aβ deposition may not be restricted to the medial temporal lobe such as hippocampus. When

comparing nondemented older subjects classified as PIB+ and PIB−, Dickerson et al. (2009) reported greater cortical thinning in the temporal pole and superior frontal cortex.

In order to delineate the relation between Aβ deposition and structural changes in normal aging, we employed voxel based morphometry (VBM), an approach that allows voxel-wise statistical analysis of pre-processed structural MR images throughout the whole brain (Ashburner & Friston, 2000, 2005; Mechelli et al., 2005). We further employed structural covariance analysis using the seed-based approach to examine a network-level neurodegenerative effect linked to amyloid deposition in clinically normal individuals.

Based on the previous findings from ROI volume approaches, we expected that Aβ deposition would be correlated with gray matter volume loss especially in hippocampus and that Aβ-dependent gray matter volume would be correlated with cognitive performance in normal aging while Aβ deposition itself as assessed with PIB PET would not, as shown in previous studies (Mormino et al., 2009).

METHODS

Subjects

Fifty-two healthy older adults (mean age = 74.1 ± 6.0 years, 34 females, mean MMSE = 29.1 ± 1.1) participated in the study. All subjects were recruited from the community via newspaper advertisements and completed PIB-PET and structural magnetic resonance imaging (MRI) scans. All subjects underwent a medical interview and a detailed battery of neuropsychological tests. In order to be eligible for the study, subjects were required to be 60 years or older, live independently in the community without neurological or psychiatric illness, and have no major medical illness or medication that influences cognition. Apolipoprotein E (APOE) ε4 carrier status was determined for older adults except for one participant using previously published methods (Agosta et al., 2009). Eighteen of the 52 older subjects in the present study also participated in our previous study examining the relationship between amyloid deposition, hippocampal volume, and episodic memory in cognitively intact older adults and MCI patients (Mormino et al., 2009). All subjects provided informed consent in accordance with the Institutional Review Boards of the University of California, Berkeley and the Lawrence Berkeley National Laboratory prior to their participation.

All subjects underwent a detailed battery of neuropsychological tests that encompass multiple cognitive domains including executive functions (e.g., Stroop test), working memory (e.g., digit span forward/backward), episodic memory (e.g., California Verbal Learning Test (CVLT) free recall, visual reproduction test), and semantic memory (e.g., vocabulary) (Table 1). In order to generate a composite score from neuropsychological tests, we utilized all test scores from a larger group of subjects who were also recruited by advertisement and underwent cognitive testing in our laboratory but did not have PIB-PET scans (N=196, mean age 72.9 years ± 7.6 years, 129 females, Mean MMSE=28.7 ± 1.7). Cognitive test scores were entered into an exploratory factor analysis with varimax rotation. Among factors extracted by the method, 5 factors that maximize the sum of variance explained were selected for the present study and based on the type of individual tests that express the highest factor loading scores for the factor, each factor was named as follows: executive function (EXE), episodic memory (EM), semantic memory (SM), working memory (WM), and visual memory (VM) (Table 1). Each subject's score for each factor (i.e., a Thompson score) was determined by regressions of a subject's raw test scores into the factor loading scores for the factor. Subjects' Thompson scores were then entered in subsequent multiple regressions to examine the relationship with gray matter volume.

In addition, 11 healthy young adults (mean age = 24.5 ± 3.5 years, 6 females, mean MMSE = 28.7 ± 1.5) were recruited from the community through online postings and underwent PIB PET, structural MRI, and neuropsychological testing. These subjects were only used to determine a cutoff score for High vs. Low Aβ burden as measured with PIB in the elderly subjects.

Imaging data acquisition

PIB—[*N*-methyl-^{11}C]-2-(4'-methylaminophenyl)-6-hydroxybenzothiazole ([^{11}C]PIB) was synthesized at the Lawrence Berkeley National Laboratory (LBNL)'s Biomedical Isotope Facility using a previously published protocol (Mathis et al., 2003). All PET scans were performed at LBNL using a Siemens ECAT EXACT HR PET scanner in three-dimensional acquisition mode. Dynamic acquisition frames (total 34 frames) were obtained over 90 minutes as follows: 4 X 15 s, 8 X 30 s, 9 X 60 s, 2 X 180 s, 8 X 300 s and 3 X 600 s. Approximately 10 to 15mCi of [^{11}C]PIB was injected as a bolus into an antecubital vein.

Structural MRI—High-resolution structural MRI scans were collected at LBNL on a 1.5 T Magnetom Avanto system (Siemens Inc., Iselin, NJ) with a 12 channel head coil run in triple mode. Three high-resolution T1-weighted magnetization-prepared rapid gradient echo (MPPAGE) scans were collected axially for each subject (TR = 2110 ms, TE = 3.58 ms, flip angle: 15°, field of view = 256 X 256 mm, matrix size: 256 X 256 mm, slices: 160, voxel size = 1 X 1 X 1 mm^3).

Imaging data analysis

PIB-PET—All PET images were preprocessed using Statistical Parametric Mapping 8 (SPM8; http://www.fil.ion.ucl.ac.uk/spm/). Region of Interest (ROI) labeling was implemented using the FreeSurfer v4.4 software package (http://surfer.nmr.mgh.harvard.edu/) in order to create a reference region in the gray matter cerebellum and to perform subsequent ROI analyses. The first five PIB frames were summed and all PIB frames including the summed image from 1–5 frames were realigned to the middle frame (17th frame). The subject's structural MRI image was coregistered to realigned PIB frames. A PIB distribution volume ratio (DVR) was calculated using Logan graphical analysis and a gray matter-masked cerebellar reference region with frames corresponding to 35–90 min post-injection (Logan et al., 1996; Price et al., 2005).

A global PIB index representing overall Aβ deposition across the brain was calculated in each subject's native space using DVR values across frontal (all frontal regions anterior to the precentral sulcus), temporal (superior, middle, and inferior temporal gyri), parietal (superior and inferior parietal cortices, supramarginal gyrus, and precuneus), and anterior/posterior cingulate cortices.

A cutoff score of the PIB index used to classify older subjects into either High or Low PIB group was calculated based on the PIB index of young adults. Older subjects were classified as in the High PIB group if their global PIB index was greater than the mean + 2 standard deviations of the PIB index of young adults. The resulting cutoff score was 1.08. As a result, 19 older subjects were classified in the High PIB group and 33 were classified in the Low PIB group. Although the cutoff score determined based on young adults' PIB indices is quite low, the proportion of older subjects who were classified in the High PIB group is about 36% of the total number of subjects. This ratio is comparable to previous reports (Bennett et al., 2006; Sperling et al., 2009).

Structural MRI—We performed VBM implemented with SPM8 running under Matlab 7.7 (Mathworks, Natick, MA) on structural images. VBM is a semi-automated procedure in

which implementation of tissue classification, bias correction, and nonlinear warping are combined. As a pre-processing step of VBM, the origin of each T1-weighted MPRAGE image of each subject was reset at the anterior commissure, followed by realignment and averaging of 3 T1-weighted MPRAGE images of each subject to yield a single high-contrast structural MRI image. The VBM procedure in the present study followed a method specified previously (Mechelli et al., 2005). Briefly, the procedure included segmentation, normalization, modulation, and smoothing steps. First, an averaged single structural T1 image for each subject was segmented into gray matter (GM), white matter (WM), and cerebral spinal fluid (CSF) using GM, WM, and CSF tissue probability maps (TPM) provided by SPM8. Segmented GM and WM were then spatially normalized to the International Consortium for Brain Mapping (ICBM) GM and WM templates using the 12-parameter affine transformation (Ashburner et al., 1997) and nonlinear registration (Ashburner & Friston, 1999). Normalized images were modulated by the Jacobian determinants derived from the normalization step in order to adjust for the resulting volume changes due to normalization (Good et al., 2001). Modulated normalized images were smoothed with a 12-mm full-width at half-maximum (FWHM) Gaussian kernel. Total intracranial volume (TIV) was calculated by summing volumes of GM, WM, and CSF derived from non-normalized segmented images. Because TIV in the present study includes CSF, it should not reflect atrophy of either GM or WM. Only voxels with a GM value greater than 0.1 (maximum value, 1) on each subject's GM were included in subsequent analyses to avoid possible edge effects around the border between GM, WM, and CSF (Sorg et al., 2007). For multiple regression analyses, we applied a threshold of $P < 0.005$, uncorrected at a voxel level. For structural covariance analyses, we applied a threshold of $P < 0.01$ corrected for multiple comparisons using the False Discovery Rate (FDR) correction method (Genovese et al., 2002).

ROI analysis

For all subjects, an averaged single structural T1 image was processed through FreeSurfer to implement region of interest (ROI) labeling. Structural images were bias field corrected, intensity normalized, and skull stripped using a watershed algorithm (Dale et al., 1999; Segonne et al., 2004). Manual touchup was performed to exclude non-brain tissue. Then, a series of image processing steps were followed: 1) these images underwent a white matter-based segmentation; 2) gray/white matter and pial surfaces were defined; and 3) topology correction was applied to these reconstructed surfaces (Dale et al., 1999; Fischl et al., 2001; Segonne et al., 2004). Subcortical and cortical ROIs spanning the entire brain were defined in each subject's native space (Fischl et al., 2002; Desikan et al., 2006). The resulting cerebellum ROI (gray matter only) was used as a reference region to create the PIB-DVR image. Resulting ROI labels were used to comprise large ROIs as stated previously.

VBM Statistical analysis

Statistical analysis was performed on the VBM-processed gray matter images using the general linear model (GLM) as implemented in SPM8. Two GLM models were constructed. First, in order to examine the regions that are negatively associated with the global PIB index across all older subjects, we constructed a multiple regression model with the global PIB index as a covariate of interest and age, gender, and TIV as covariates that are controlled for. Second, in order to examine the regions that are negatively associated with the global PIB index only in the High PIB group, we constructed the same multiple regression model except for the number of subjects included (i.e., only 19 subjects were in this model). The resulting statistical maps were thresholded at $p < .005$ uncorrected for multiple comparison correction.

Structural covariance analysis

In order to further probe regions whose gray matter volumes covary together, we applied structural covariance analysis as employed in Mechelli et al. (2005) and adapted in Seeley et al. (2009). First, we made a spherical ROI with a 4-mm radius centering on the peak coordinates resulting from the 2 multiple regression analyses as described in the previous section. These spherical ROIs served as "seed regions" in the following structural covariance analyses. We extracted the local densities from these 2 seed regions of interest in the VBM-processed gray matter images of all older subjects and used these values as predictors of regional densities in all voxels of the VBM-processed gray matter images. All areas of the cortex that showed a positive correlation with the seed regions were included in the resulting structural covariance maps. To remove any pattern of covariance that could be attributed to age and gender effects, we added age and gender into the model as covariates to be controlled for. In addition, the TIV in each subject was entered as a confounding variable to identify brain regions in which gray matter volume changes were not explained by global brain size measures as indicated in TIV. Adding TIV as a covariate of no interest was especially important considering the fact that, although insignificant, there was a trend of larger TIV for the low PIB group than the high PIB group as reported in the results section. Therefore, 2 structural covariance maps were generated: one with a seed region determined based on all older subjects and the other with a seed region based on only High PIB subjects. Our models were set in order to ensure identifying voxels in which gray matter volume covaries positively with our seed regions regardless of age, gender, and brain size as measured in TIV. The resulting statistical maps were thresholded at $p < .01$, and corrected for multiple comparisons (voxel-level control of FDR).

Multiple regressions with cognitive test scores

All non-image analyses were conducted using SPSS software (version 17). Differences between High and Low PIB groups for gender and APOE genotypes were assessed by χ^2 tests. Independent sample t-tests were used to compare means between High and Low PIB groups. Multiple regressions were used to assess the relationship between global PIB index and cognitive performance and between gray matter volume and cognitive performance. These analyses resulted in a total of 10 multiple regressions for a combination of 5 cognitive factors as dependent measures and 2 predictors of interest (i.e., a global PIB index and gray matter volume). Age, gender, and education were controlled in all analyses. TIV was further controlled in analyses involving gray matter volume as a predictor of interest. Statistical significance was determined at $\alpha = .05$, two-tailed.

RESULTS

Characteristics of participants

Demographics, global PIB index, and Mini Mental State Examination (MMSE) scores for older subjects are summarized in Table 2. High PIB vs. Low PIB groups did not differ on any measures such as age, gender, education, APOE genotypes, and MMSE. Although it was not statistically significant, there was a trend for larger TIV in the Low PIB group compared to the High PIB group (Low PIB: 1617.4 ± 177.4; High PIB: 1533.0 ± 121.2, $p = .07$). There was no significant difference in PIB index between Low PIB group and young subjects (Low PIB: 1.02 ± 0.03; Young: 1.01 ± 0.04, $p > .2$).

Factor scores and raw scores of neuropsychological tests were compared between high PIB and low PIB groups by independent sample t-tests. There was no significant difference between high PIB and low PIB groups on any factors and raw scores (ps > .1) (Table 3).

Relationships between PIB index and gray matter volume in normal aging

Across all 52 subjects, decreased gray matter volume in association with a higher global PIB index was found in the left inferior frontal gyrus (IFG; peak coordinates: X = −44, Y = 12, Z = 14) ($p < .005$ uncorrected) (Figure 1A).

Across 19 subjects who were classified in the high PIB group, voxel-wise multiple regression with the global PIB index as a predictor of interest revealed the posterior cingulate cortex (PCC; peak coordinates: X = −10, Y = −38, Z = 30) as the region showing the strongest association between PIB index and gray matter volume loss ($p < .005$ uncorrected) (Figure 2A).

Additional analyses were performed by adding APOE genotypes as a covariate in the previously specified GLM models. The addition of APOE genotypes as a covariate, however, did not change the results.

Structural covariance pattern associated with a seed region defined by its association with PIB index

When peak coordinates of the left IFG region were used as a seed, widespread frontal regions including the inferior frontal gyrus bilaterally, orbital and medial frontal gyrus showed significant covariation (Figure 1B). When peak coordinates of the PCC that showed reduced gray matter volume only in the high PIB group were used as a seed region for structural covariance analysis, widespread regions including medial frontal cortex, lateral parietal cortex, posterior hippocampus, and precuneus significantly covaried (Figure 2B).

Relationship between gray matter volume loss and cognitive performance

We examined the association between Aβ-dependent gray matter volume changes and cognitive performance. Gray matter volume in the left IFG – seeded network was positively associated with the factor score of working memory across all subjects. This result was significant with participants' age, gender, education, and TIV being covaried out (standardized $\beta = .477$, $p = .035$, without multiple comparison correction). Figure 3 illustrates the relationship of frontal network grey matter volume and working memory performance for the whole group, high PIB group, and low PIB group. Gray matter volume in the PCC – seeded network, however, was not associated with any cognitive measures. Resulting β values from all multiple regression models are listed in Table 4.

Relationship between PIB index and cognitive performance

To test whether there is a significant relationship between Aβ deposition and cognitive performance in normal aging, we examined the association between PIB index and cognitive performance as indicated in the 5 factor scores. As previously reported (Aizenstein et al., 2008; Mormino et al., 2009), we did not find any significant relationship between two measures (Table 4).

DISCUSSIONS

In the present study, we aimed to characterize the relationship between Aβ deposition and gray matter volume, to examine the association of Aβ with cognitive performance, and to examine the association of Aβ-dependent gray matter volume changes with cognitive performance in normal aging. Across all older subjects, we found that gray matter volume in the left IFG was negatively associated with Aβ deposition. With only High PIB older subjects, a negative association between gray matter volume and PIB index was found in the PCC. When these two brain regions were used as seed regions, structural covariance analysis revealed dissociated brain networks (Figure 4). The left IFG – seeded network

involved mainly the lateral frontal cortex whereas the PCC – seeded network involved widespread regions including precuneus, parietal cortex, temporal cortex, anterior cingulate, medial frontal cortex, and hippocampus. When we related gray matter volume in these two distinct networks to cognitive performance, gray matter volume in the left IFG – seeded network was associated with working memory performance. Neither Aβ deposition itself nor gray matter volume in the PCC – seeded network was associated with any cognitive measures.

Aβ deposition and gray matter volume reduction in normal aging

Previous studies have indicated that a fairly large proportion of cognitively normal older people exhibit elevated Aβ deposition measured by PIB PET and some have suggested the possibility that these elderly people have a higher risk of developing AD (Aizenstein et al., 2008; Pike et al., 2007). In a longitudinal study, Storandt et al. (2009) have shown the negative cognitive and structural consequences of Aβ levels in cognitively healthy older adults. In a cross-sectional study, Aβ deposition was inversely related to hippocampal volume which was shown to mediate an influence of Aβ deposition on episodic memory performance (Mormino et al., 2009). Taken together, Aβ deposition and gray matter volume seem to be correlated both longitudinally and cross-sectionally in normal elderly individuals.

When we examined whole brain gray matter volume in association with Aβ deposition only in the High PIB group, the PCC emerged as a region that is most negatively affected by Aβ deposition. The brain network structurally covarying with this region in terms of gray matter volume included the hippocampus, precuneus, medial frontal cortex, anterior cingulate gyrus, and temporal and parietal cortices. Our results revealed by structural covariance analysis are consistent with recent findings showing that Aβ deposition is negatively associated with gray matter volume in posterior cingulate, anterior cingulate, temporal cortex, and hippocampus (Chetelat et al., 2010; Storandt et al., 2009). Notably, this PCC – seeded network resembles the DMN which has been suggested to be disrupted as a function of Aβ deposition in both AD and normal aging. Using fMRI studies of resting state connectivity, Hedden et al. (2009) showed that the DMN including the precuneus/posterior cingulate is more disrupted in nondemented elderly who are PIB+ than those who are PIB−. They further showed that the functional correlation between the precuneus/posterior cingulate and hippocampus is significantly lower in the group of PIB+ than PIB− subjects. Thus, the current findings of overlapping topography of reduced gray matter volume and the default network clearly suggest that functionally connected brain regions may share anatomical changes as well.

Although a central role of the medial temporal lobe in episodic memory and its volume loss in association with Aβ deposition are previously reported, a relationship between frontal gray matter volume and Aβ deposition is a new finding in the present study. The frontal network in association with Aβ deposition was identified by applying a structural covariance method with a seed region of the left IFG whose gray matter volume was negatively correlated with Aβ deposition in the entire sample. Dysfunction of the left IFG, however, has been implicated as an earlier manifestation of Alzheimer's disease using fMRI. Bookheimer et al. (2000) have shown that the initial extent of activation in the left IFG predicted memory decline in the domain of episodic memory in normal elderly who carry the APOE ε4 allele and thus are genetically at risk for AD. Although the imaging modality that we used to probe this region in association with Aβ deposition is different from that of Bookheimer et al.'s (2000), the current finding is consistent with theirs in suggesting that the left IFG is affected in presymptomatic status of AD. In order to directly relate the present findings to those of Bookheimer et al.'s (2000), it will be necessary to examine whether compensatory functional changes occur in the regions suffering neurodegeneration in association with Aβ deposition by using other imaging modalities such as FDG PET.

Association of Aβ deposition and gray matter volume with cognitive performance

In this study, we did not find an association between Aβ deposition and cognitive performance. This finding is consistent with previous reports showing no relationship between Aβ deposition and cognitive performance within each pathologically distinct group (i.e., normal older subjects vs. MCI vs. AD) (Aizenstein et al., 2008; Mormino et al., 2009; Rowe et al., 2007). Some studies, however, have indicated that the relationship between Aβ deposition and cognitive performance is mediated by other structural and/or functional factors. Mormino et al. (2009) have shown a mediating role of hippocampal volume on the relationship between Aβ deposition and episodic memory performance. As indicated in Storandt et al. (2009), baseline Aβ deposition further can be associated with cognitive changes over time, although it is unclear whether this longitudinal change in cognition is also mediated by concurrent gray matter volume change as a function of Aβ deposition (Scheinin et al., 2009). Therefore, the current findings are consistent with the idea that deterioration of cognitive functions may be more affected by neuronal changes such as neuronal or synaptic loss resulting in gray matter volume loss, rather than Aβ burden itself. The continued presence of a given amount of Aβ may progressively destroy neural function and lead to deterioration of cognition as implicated in the Aβ cascade hypothesis (Jack et al., 2010).

We found dissociation between the frontal and posterior networks on cognitive performance. The frontal network gray matter volume was positively associated with working memory performance in all older subjects while the posterior network was not associated with any cognitive measures examined in the present study. The medial temporal lobe and precuneus, which have been postulated as regions showing significant gray matter volume loss in association with Aβ deposition in both AD and normal aging, are frequently shown to be related to episodic memory disturbance in these populations (e.g., Mormino et al., 2009). The lack of association between the posterior network gray matter volume and cognitive performance may be due to the fact that the posterior network identified in this study included much broader regions beyond the medial temporal lobe and precuneus. Indeed, when we examined an association between factor scores of episodic memory and right hippocampal gray matter volume (i.e., VBM data masked by MNI-based right hippocampus ROI), there was a significant positive association between these two variables while age, gender, education, and TIV were controlled for ($\beta = .445$, $p < .05$). This finding is quite consistent with our previous reports (Mormino et al., 2009), although we previously found a significant association between episodic memory and hippocampal volume bilaterally, while we found a significant association between episodic memory and right hippocampal volumes only in the present study. In addition, although voxel-wise whole brain analysis did not reveal a significant association between hippocampus and PIB index, the structural covariance pattern using the PCC seed revealed that the degree of gray matter volume of hippocampus bilaterally fluctuates in the same manner with that of the PCC. Therefore, two lines of evidence seem to support the generalizability of our previous reports.

In the present study, we found the frontal network in association with the PIB index across all subjects while the DMN was associated with the PIB index only in the high PIB subjects. The present findings are quite similar to Wolk et al.'s (2010) that showed dissociation between frontal and posterior networks mediated by APOE. They found greater cortical thinning in the frontoparietal regions in noncarriers of ε4 alleles of APOE genotype while greater cortical thinning in the medial temporal lobe in APOE ε4 carriers. In addition, worse performance in working memory, executive functions, and lexical access was observed in noncarriers whereas poorer episodic memory was seen in carriers. Examination of the effect of APOE genotypes in our study, however, did not reveal this type of dissociation. One potential explanation for the lack of association between genotypes and gray matter volume changes in the present study might be that our sample is not large enough to investigate this

relationship, because there were about 70 APOE ε4 carriers (among them, 34% homozygotes) in Wolk et al. (2010) while our sample includes only 16 APOE ε4 carriers (13% homozygotes). Another possibility is that, while participants in Wolk et al. (2010) were AD patients, our subjects are clinically normal elderly. We screened out older subjects whose cognitive performance in various domains falls 2 standard deviations below the mean of age, education, and gender adjusted normed data in addition to MMSE cutoff scores (≥ 26). Therefore, the lack of association between genotypes and gray matter volume changes in the present study may further indicate that the degree of the structural brain phenotype associated with APOE genotype could be different between clinical and preclinical populations.

The frontal network identified in the current study overlaps with that in previous findings indicating aging-related frontal gray matter reduction during normal aging (Raz et al., 1997, 1999). Because this network was seen in an analysis controlling for the effect of age, it is possible that there is an additional effect of Aβ deposition on gray matter volume changes in this network. The association of the frontal network gray matter volume with working memory performance further suggests functional consequences for this pattern of atrophy in aging and is consistent with known neuroanatomical and behavioral correlates (Goldman-Rakic, 1987; Raz et al., 1999). The posterior network, on the other hand, seems to be affected at a more advanced stage of Aβ deposition in cognitively intact older people. We found no association of posterior network gray matter volume with cognition, although our null findings are limited to structural changes in this network. More investigation is warranted to elucidate the role of the posterior network in cognition during normal aging.

CONCLUSIONS

Although cognitively normal, older subjects experience varying levels of β-amyloid deposition which is a hallmark of AD pathology. Results from the present study highlight structural and cognitive changes in association with the level of Aβ deposition in cognitively intact normal elderly. We identify two brain networks in which the degree of gray matter volume fluctuates in a similar manner: a frontal network and a posterior network. Gray matter volume in the frontal network was shown to be associated with working memory performance whereas no significant association with cognitive measures was found for the posterior network. Findings from the present study suggest that β-amyloid deposition in older people without dementia may influence a wide structural network, although we do not know whether people with higher β-amyloid deposition will progress to AD. Studies with a larger sample and longitudinal studies will be necessary to shed light on the longitudinal effect of β-amyloid deposition observed in normal aging.

References

Agosta F, Vossel KA, Miller BL, Migliaccio R, Bonasera SJ, Filippi M, et al. Apolipoprotein E epsilon4 is associated with disease-specific effects on brain atrophy in Alzheimer's disease and frontotemporal dementia. Proc Natl Acad Sci U S A 2009;106(6):2018–2022. [PubMed: 19164761]

Aizenstein HJ, Nebes RD, Saxton JA, Price JC, Mathis CA, Tsopelas ND, et al. Frequent amyloid deposition without significant cognitive impairment among the elderly. Arch Neurol 2008;65(11): 1509–1517. [PubMed: 19001171]

Archer HA, Edison P, Brooks DJ, Barnes J, Frost C, Yeatman T, et al. Amyloid load and cerebral atrophy in Alzheimer's disease: an 11C-PIB positron emission tomography study. Ann Neurol 2006;60(1):145–147. [PubMed: 16802294]

Ashburner J, Friston KJ. Nonlinear spatial normalization using basis functions. Hum Brain Mapp 1999;7(4):254–266. [PubMed: 10408769]

Ashburner J, Friston KJ. Voxel-based morphometry--the methods. Neuroimage 2000;11(6):805–821. [PubMed: 10860804]

Ashburner J, Friston KJ. Unified segmentation. Neuroimage 2005;26(3):839–851. [PubMed: 15955494]

Ashburner J, Neelin P, Collins DL, Evans A, Friston K. Incorporating prior knowledge into image registration. Neuroimage 1997;6(4):344–352. [PubMed: 9417976]

Bobinski M, de Leon MJ, Wegiel J, Desanti S, Convit A, Saint Louis LA, et al. The histological validation of post mortem magnetic resonance imaging-determined hippocampal volume in Alzheimer's disease. Neuroscience 2000;95(3):721–725. [PubMed: 10670438]

Bookheimer SY, Strojwas MH, Cohen MS, Saunders AM, Pericak-Vance MA, Mazziotta JC, et al. Patterns of brain activation in people at risk for Alzheimer's disease. N Engl J Med 2000;343(7): 450–456. [PubMed: 10944562]

Bourgeat P, Chetelat G, Villemagne VL, Fripp J, Raniga P, Pike K, et al. Betaamyloid burden in the temporal neocortex is related to hippocampal atrophy in elderly subjects without dementia. Neurology 2010;74(2):121–127. [PubMed: 20065247]

Braak H, Braak E. Demonstration of amyloid deposits and neurofibrillary changes in whole brain sections. Brain Pathol 1991;1(3):213–216. [PubMed: 1669710]

Buckner RL, Snyder AZ, Shannon BJ, LaRossa G, Sachs R, Fotenos AF, et al. Molecular, structural, and functional characterization of Alzheimer's disease: evidence for a relationship between default activity, amyloid, and memory. J Neurosci 2005;25(34):7709–7717. [PubMed: 16120771]

Chetelat G, Villemagne VL, Bourgeat P, Pike KE, Jones G, Ames D, et al. Relationship between atrophy and beta-amyloid deposition in Alzheimer disease. Ann Neurol 2010;67(3):317–324. [PubMed: 20373343]

Csernansky JG, Hamstra J, Wang L, McKeel D, Price JL, Gado M, et al. Correlations between antemortem hippocampal volume and postmortem neuropathology in AD subjects. Alzheimer Dis Assoc Disord 2004;18(4):190–195. [PubMed: 15592129]

Dale AM, Fischl B, Sereno MI. Cortical surface-based analysis. I. Segmentation and surface reconstruction. Neuroimage 1999;9(2):179–194. [PubMed: 9931268]

de Leon MJ, George AE, Stylopoulos LA, Smith G, Miller DC. Early marker for Alzheimer's disease: the atrophic hippocampus. Lancet 1989;2(8664):672–673. [PubMed: 2570916]

Desikan RS, Segonne F, Fischl B, Quinn BT, Dickerson BC, Blacker D, et al. An automated labeling system for subdividing the human cerebral cortex on MRI scans into gyral based regions of interest. Neuroimage 2006;31(3):968–980. [PubMed: 16530430]

Dickerson BC, Bakkour A, Salat DH, Feczko E, Pacheco J, Greve DN, et al. The cortical signature of Alzheimer's disease: regionally specific cortical thinning relates to symptom severity in very mild to mild AD dementia and is detectable in asymptomatic amyloid-positive individuals. Cereb Cortex 2009;19(3):497–510. [PubMed: 18632739]

Fischl B, Liu A, Dale AM. Automated manifold surgery: constructing geometrically accurate and topologically correct models of the human cerebral cortex. IEEE Trans Med Imaging 2001;20(1): 70–80. [PubMed: 11293693]

Fischl B, Salat DH, Busa E, Albert M, Dieterich M, Haselgrove C, et al. Whole brain segmentation: automated labeling of neuroanatomical structures in the human brain. Neuron 2002;33(3):341–355. [PubMed: 11832223]

Fotenos AF, Snyder AZ, Girton LE, Morris JC, Buckner RL. Normative estimates of cross-sectional and longitudinal brain volume decline in aging and AD. Neurology 2005;64(6):1032–1039. [PubMed: 15781822]

Genovese CR, Lazar NA, Nichols T. Thresholding of statistical maps in functional neuroimaging using the false discovery rate. Neuroimage 2002;15(4):870–878. [PubMed: 11906227]

Goldman-Rakic, PS. Circuitry of primate prefrontal cortex and regulation of behavior by representational memory. In: Mountcastle, VB.; Plum, F., editors. Handbook of physiology: The nervous system, higher functions of the brain. Vol. Vol. 5. Bethesda, MD: American Physiological Society; 1987. p. 373-417.

Good CD, Johnsrude IS, Ashburner J, Henson RN, Friston KJ, Frackowiak RS. A voxel-based morphometric study of ageing in 465 normal adult human brains. Neuroimage 2001;14(1):21–36. [PubMed: 11525331]

Greicius MD, Srivastava G, Reiss AL, Menon V. Default-mode network activity distinguishes Alzheimer's disease from healthy aging: evidence from functional MRI. Proc Natl Acad Sci U S A 2004;101(13):4637–4642. [PubMed: 15070770]

Hardy J, Selkoe DJ. The amyloid hypothesis of Alzheimer's disease: progress and problems on the road to therapeutics. Science 2002;297(5580):353–356. [PubMed: 12130773]

Hedden T, Van Dijk KR, Becker JA, Mehta A, Sperling RA, Johnson KA, et al. Disruption of functional connectivity in clinically normal older adults harboring amyloid burden. J Neurosci 2009;29(40):12686–12694. [PubMed: 19812343]

Ikonomovic MD, Klunk WE, Abrahamson EE, Mathis CA, Price JC, Tsopelas ND, et al. Post-mortem correlates of in vivo PiB-PET amyloid imaging in a typical case of Alzheimer's disease. Brain 2008;131(6):1630–1645. [PubMed: 18339640]

Jack CR Jr, Dickson DW, Parisi JE, Xu YC, Cha RH, O'Brien PC, et al. Antemortem MRI findings correlate with hippocampal neuropathology in typical aging and dementia. Neurology 2002;58(5): 750–757. [PubMed: 11889239]

Jack CR Jr, Knopman DS, Jagust WJ, Shaw LM, Aisen PS, Weiner MW, et al. Hypothetical model of dynamic biomarkers of the Alzheimer's pathological cascade. Lancet Neurol 2010;9(1):119–128. [PubMed: 20083042]

Jack CR Jr, Lowe VJ, Senjem ML, Weigand SD, Kemp BJ, Shiung MM, et al. 11C PiB and structural MRI provide complementary information in imaging of Alzheimer's disease and amnestic mild cognitive impairment. Brain 2008;131(3):665–680. [PubMed: 18263627]

Jack CR Jr, Lowe VJ, Weigand SD, Wiste HJ, Senjem ML, Knopman DS, et al. Serial PIB and MRI in normal, mild cognitive impairment and Alzheimer's disease: implications for sequence of pathological events in Alzheimer's disease. Brain 2009;132(5):1355–1365. [PubMed: 19339253]

Klunk WE, Engler H, Nordberg A, Wang Y, Blomqvist G, Holt DP, et al. Imaging brain amyloid in Alzheimer's disease with Pittsburgh Compound-B. Ann Neurol 2004;55(3):306–319. [PubMed: 14991808]

Klunk WE, Wang Y, Huang GF, Debnath ML, Holt DP, Shao L, et al. The binding of 2-(4'-methylaminophenyl)benzothiazole to postmortem brain homogenates is dominated by the amyloid component. J Neurosci 2003;23(6):2086–2092. [PubMed: 12657667]

Logan J, Fowler JS, Volkow ND, Wang GJ, Ding YS, Alexoff DL. Distribution volume ratios without blood sampling from graphical analysis of PET data. J Cereb Blood Flow Metab 1996;16(5):834–840. [PubMed: 8784228]

Mathis CA, Wang Y, Holt DP, Huang GF, Debnath ML, Klunk WE. Synthesis and evaluation of 11C-labeled 6-substituted 2-arylbenzothiazoles as amyloid imaging agents. J Med Chem 2003;46(13): 2740–2754. [PubMed: 12801237]

Mechelli A, Friston KJ, Frackowiak RS, Price CJ. Structural covariance in the human cortex. J Neurosci 2005;25(36):8303–8310. [PubMed: 16148238]

Mechelli A, Price CJ, Friston KJ, Ashburner J. Voxel-based morphometry of the human brain: methods and applications. Current Medical Imaging Reviews 2005;1:105–113.

Mintun MA, Larossa GN, Sheline YI, Dence CS, Lee SY, Mach RH, et al. [11C]PIB in a nondemented population: potential antecedent marker of Alzheimer disease. Neurology 2006;67(3):446–452. [PubMed: 16894106]

Mormino EC, Kluth JT, Madison CM, Rabinovici GD, Baker SL, Miller BL, et al. Episodic memory loss is related to hippocampal-mediated beta-amyloid deposition in elderly subjects. Brain 2009;132(5):1310–1323. [PubMed: 19042931]

Pike KE, Savage G, Villemagne VL, Ng S, Moss SA, Maruff P, et al. Beta-amyloid imaging and memory in non-demented individuals: evidence for preclinical Alzheimer's disease. Brain 2007;130(11):2837–2844. [PubMed: 17928318]

Price JC, Klunk WE, Lopresti BJ, Lu X, Hoge JA, Ziolko SK, et al. Kinetic modeling of amyloid binding in humans using PET imaging and Pittsburgh Compound-B. J Cereb Blood Flow Metab 2005;25(11):1528–1547. [PubMed: 15944649]

Raz N, Briggs SD, Marks W, Acker JD. Age-related deficits in generation and manipulation of mental images: II. The role of dorsolateral prefrontal cortex. Psychol Aging 1999;14(3):436–444. [PubMed: 10509698]

Raz N, Gunning FM, Head D, Dupuis JH, McQuain J, Briggs SD, et al. Selective aging of the human cerebral cortex observed in vivo: differential vulnerability of the prefrontal gray matter. Cereb Cortex 1997;7(3):268–282. [PubMed: 9143446]

Reiman EM, Chen K, Liu X, Bandy D, Yu M, Lee W, et al. Fibrillar amyloid-beta burden in cognitively normal people at 3 levels of genetic risk for Alzheimer's disease. Proc Natl Acad Sci U S A 2009;106(16):6820–6825. [PubMed: 19346482]

Rowe CC, Ng S, Ackermann U, Gong SJ, Pike K, Savage G, et al. Imaging beta-amyloid burden in aging and dementia. Neurology 2007;68(20):1718–1725. [PubMed: 17502554]

Scheinin NM, Aalto S, Koikkalainen J, Lotjonen J, Karrasch M, Kemppainen N, et al. Follow-up of [11C]PIB uptake and brain volume in patients with Alzheimer disease and controls. Neurology 2009;73(15):1186–1192. [PubMed: 19726751]

Seeley WW, Crawford RK, Zhou J, Miller BL, Greicius MD. Neurodegenerative diseases target large-scale human brain networks. Neuron 2009;62(1):42–52. [PubMed: 19376066]

Segonne F, Dale AM, Busa E, Glessner M, Salat D, Hahn HK, et al. A hybrid approach to the skull stripping problem in MRI. Neuroimage 2004;22(3):1060–1075. [PubMed: 15219578]

Silbert LC, Quinn JF, Moore MM, Corbridge E, Ball MJ, Murdoch G, et al. Changes in premorbid brain volume predict Alzheimer's disease athology. Neurology 2003;61(4):487–492. [PubMed: 12939422]

Sorg C, Riedl V, Muhlau M, Calhoun VD, Eichele T, Laer L, et al. Selective changes of resting-state networks in individuals at risk for Alzheimer's disease. Proc Natl Acad Sci U S A 2007;104(47): 18760–18765. [PubMed: 18003904]

Sperling RA, Laviolette PS, O'Keefe K, O'Brien J, Rentz DM, Pihlajamaki M, et al. Amyloid deposition is associated with impaired default network function in older persons without dementia. Neuron 2009;63(2):178–188. [PubMed: 19640477]

Storandt M, Mintun MA, Head D, Morris JC. Cognitive decline and brain volume loss as signatures of cerebral amyloid-beta peptide deposition identified with Pittsburgh compound B: cognitive decline associated with Abeta deposition. Arch Neurol 2009;66(12):1476–1481. [PubMed: 20008651]

Wolk DA, Dickerson BC, Weiner M, Aiello M, Aisen P, Albert MS, et al. Apolipoprotein E (APOE) genotype has dissociable effects on memory and attentional-executive network function in Alzheimer's disease. Proc Natl Acad Sci US A 2010;107(22):10256–10261.

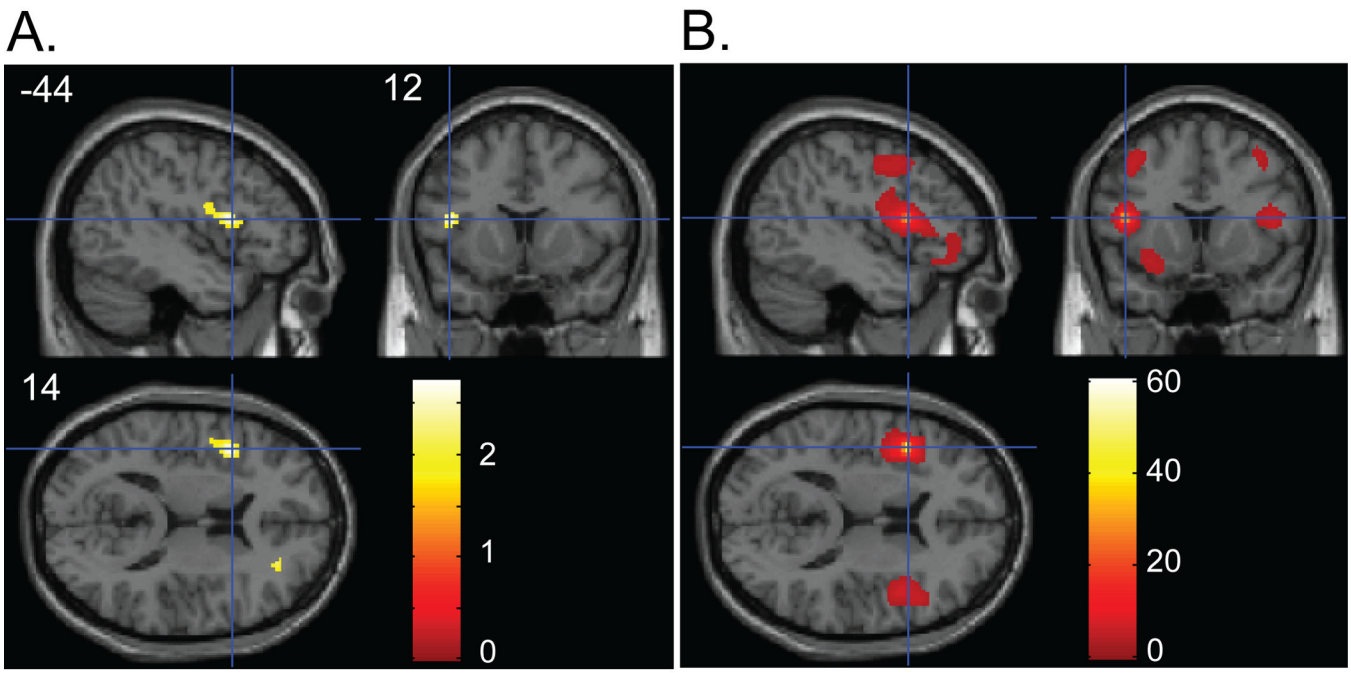

Figure 1.

(A) Regions showing a negative association between gray matter volume and PIB index. Panel shows sagittal, coronal and axial slices in MNI space with a cross hair marking the location of the average peak coordinate as indicated by numbers (X = −44, Y = 12, Z = 14) in mm. Age, gender, and TIV were controlled for. Threshold at $p < .05$ (uncorrected) is used for visualization. (B) Structural covariance pattern that fluctuates with gray matter density in the left IFG. Panel shows sagittal, coronal and axial slices with a cross hair marking the location of the seed region (i.e., left IFG). Age, gender, and TIV were controlled for. The map was thresholded at $p < .01$ with multiple comparison correction (FDR). The color bars represent T-values.

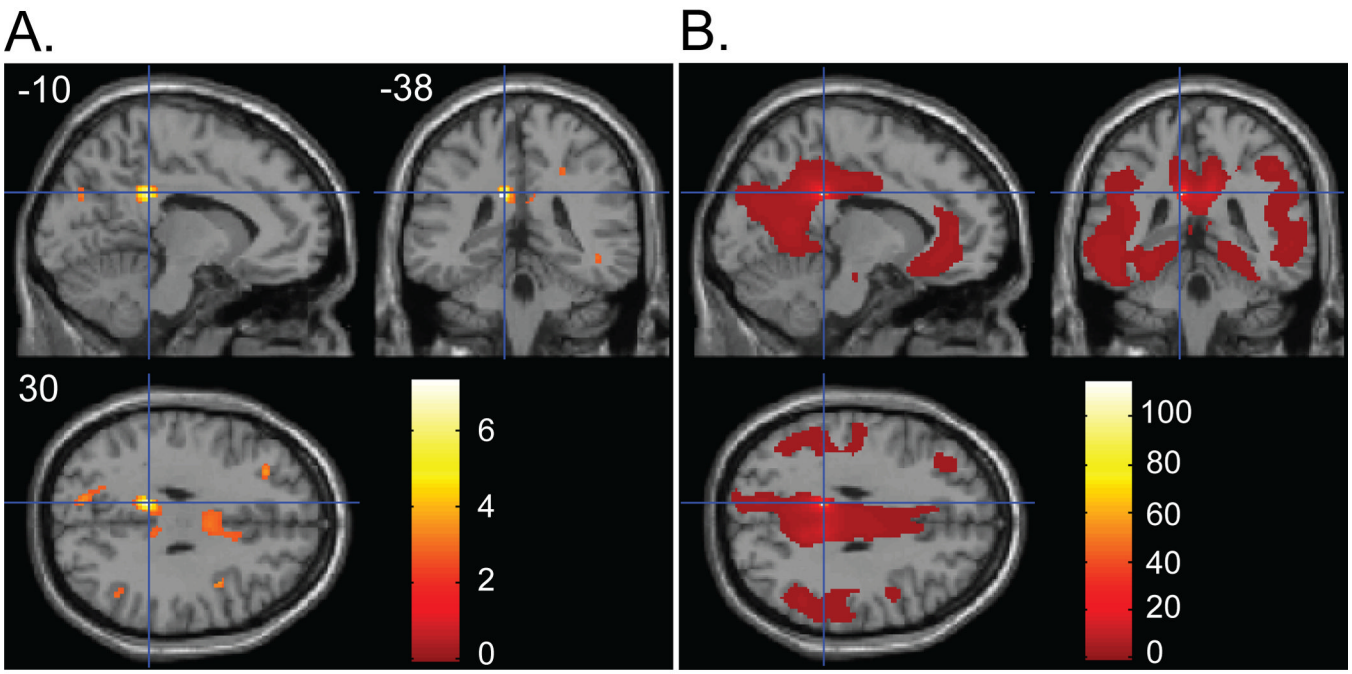

Figure 2.

(A) Regions showing a negative association between gray matter volume and PIB index in High PIB group. Panel shows sagittal, coronal and axial slices in MNI space with a cross hair marking the location of the average peak coordinate as indicated by numbers (X = −10, Y = −38, Z = 30) in mm. Age, gender, and TIV were controlled for. Threshold at p<. 01(uncorrected) is used for visualization. (B) Structural covariance pattern that fluctuates with gray matter density in the PCC. Panel shows sagittal, coronal and axial slices with a cross hair marking the location of the seed region (i.e., PCC). Age, gender, and TIV were controlled for. The map was thresholded at p<.01 with multiple comparison correction (FDR). The color bars represent T-values.

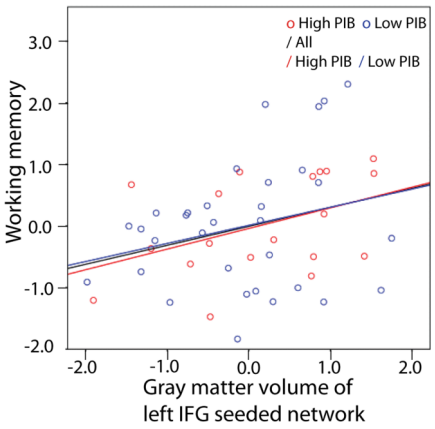

Figure 3.

A partial correlation scatterplot illustrating the relationship of frontal network grey matter volume and working memory performance for the whole group, high PIB group, and low PIB group. The x-axis of the scatterplot represents standardized residuals of frontal network grey matter volume and the y-axis represents standardized residuals of working memory factor scores. For both standardized residual measures, age, gender, education, and TIV were regressed out. The trend of the relationship between frontal gray matter volume and working memory performance is the same across all participants regardless of their PIB group membership. High PIB group: R = .432, p = .065; Low PIB group: R = .257, p = .156; Whole group: R = .308, p = .028.

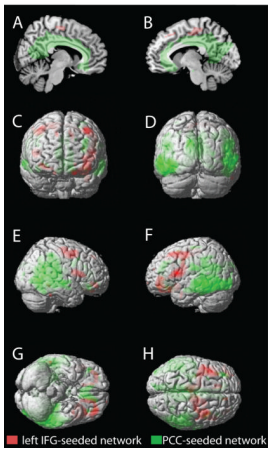

Figure 4.

Dissociation of the left IFG – seeded network and the PCC – seeded network. Group composite maps are shown on the medial view of right and left hemispheres (A and B), the anterior and posterior surfaces (C and D), the right and left lateral surfaces (E and F), and the ventral and dorsal surfaces (G and H) of the rendered MNI single-subject brain. Regions in red and green indicate suprathreshold voxels identified by structural covariance analysis with the left IFG seed ("left IFG - seeded network") and the PCC seed ("PCC – seeded network"), respectively. Maps were thresholded at $p < .01$, corrected for multiple comparisons (voxel-level FDR).

Table 1

Factor loadings of individual cognitive measures contributing to each factor

	Factor loadings				
Neuropsychological tests	**EXE**	**EM**	**SM**	**WM**	**VM**
CVLT immediate recall	0.34	**0.74**	0.09	0.13	0.13
CVLT delayed recall	0.24	**0.96**	0.10	0.02	0.09
CVLT recognition	0.24	**0.79**	0.07	0.03	0.12
Digit span forward	0.13	0.09	0.14	**0.72**	0.04
Digit span backward	0.21	−0.01	0.16	**0.69**	0.06
Listening span	**0.58**	0.32	0.18	**0.52**	0.12
Boston naming	−0.05	0.07	**0.56**	0.12	0.10
Vocabulary	0.15	0.10	**0.96**	0.18	−0.06
Stroop	**0.67**	0.21	0.05	0.17	0.07
Trail A	**0.59**	0.15	−0.06	0.11	0.19
Digit symbol	**0.82**	0.27	0.03	0.13	0.09
Visual reproduction immediate recall	**0.53**	0.28	0.15	0.13	**0.77**
Visual reproduction delayed recall	**0.58**	0.39	0.04	0.08	**0.48**

Factor loadings of neuropsychological tests listed under each factor in Table 3 are bold-faced. EXE: executive functions; EM: episodic memory; SM: semantic memory; WM: working memory; VM: visual memory; CVLT: California Verbal Learning Test

Table 2

Characteristics of participants

	Total (n = 52)		Low PIB (n = 33)		High PIB (n = 19)	
	M	**SD**	**M**	**SD**	**M**	**SD**
Age (yrs)	74.11	6.02	73.93	5.73	74.41	6.64
Education (yrs)	17.21	1.93	17.45	1.84	16.79	2.07
Gender (n, F/M)[a]	34/18		20/13		14/5	
PIB index	1.12	0.19	1.02	0.03	1.28	0.24
APOE-ε4 (n[%])[b]	16 (31%)		8 (24.2%)		8 (44.4%)	
TIV	1586.56	163.16	1617.43	177.44	1532.95	121.13
MMSE	29.08	1.07	29.00	1.16	29.21	0.92

[a] χ^2 =.911, p > .1

[b] Proportion of individuals with APOE genotypes ε3/4 or ε4/4, χ^2 = 2.208, p > .1

TIV: total intracranial volume; PIB: Pittsburgh compound B; MMSE: Mini-Mental State Examination

Table 3

Major individual cognitive measures constituting each factor and factor scores between High PIB and Low PIB groups

***Factors*/Cognitive tests**	***Factor*/Raw test scores**			
	Low PIB		**High PIB**	
	M	**SD**	**M**	**SD**
Executive functions	*−0.30*	*0.63*	*−0.31*	*0.68*
Stroop	49.00	11.73	50.84	12.65
Trail A	36.14	10.02	37.62	14.39
Digit symbol	61.55	9.17	63.11	12.84
Listening span	47.31	7.78	46.16	9.66
Visual reproduction immediate recall	82.00	11.94	77.84	13.76
Visual reproduction delayed recall	67.31	17.25	58.16	24.27
Episodic memory	*−0.05*	*1.05*	*−0.21*	*1.09*
CVLT immediate recall	50.28	9.98	49.26	13.35
CVLT delayed recall	11.53	3.02	11.11	3.91
CVLT recognition	13.6	2.08	12.8	3.20
Semantic memory	*0.35*	*0.75*	*0.03*	*0.58*
Boston naming	14.79	0.41	14.47	0.90
Vocabulary	58.85	5.93	56.51	5.45
Working memory	*−0.18*	*0.90*	*−0.19*	*0.67*
Digit span forward	9.50	2.48	10.21	1.93
Digit span backward	7.91	2.51	6.89	1.82
Listening span	47.31	7.78	46.16	9.66
Visual memory	*0.06*	*1.15*	*−0.24*	*1.07*
Visual reproduction immediate recall	82.00	11.94	77.84	13.76
Visual reproduction delayed recall	67.31	17.25	58.16	24.27

Two-sample T-tests did not reveal any significant difference for both raw neuropsychological test measures and 5 factor scores between High PIB and Low PIB groups. CVLT: California Verbal Learning Test

Table 4

Matrix of standardized beta values for all multiple regression models

Factors	PIB index[a]	Frontal gray matter volume[b]	Posterior gray matter volume[b]
EXE	0.007	0.003	−0.174
EM	−0.003	0.216	0.069
SM	−0.203	−0.202	−0.049
WM	0.033	**0.477**	0.282
VM	−0.126	−0.003	−0.018

Significant beta values of multiple regressions are bold-faced.

[a] Multiple regression models included age, gender, and education as covariates of no interest.

[b] Multiple regression models included age, gender, education, and TIV as covariates of no interest.

EXE: executive functions; EM: episodic memory; SM: semantic memory; WM: working memory; VM: visual memory